Available online at www.elixirpublishers.com (Elixir International Journal)

Corrosion and Dye

Elixir Corrosion & Dye 77 (2014) 28958-28967

ISSN: 2229-712X

Synthesis of a new type of cationic surfactants and evaluation of their performance as corrosion inhibitors for X-65 tubing steel under H_2S environment

M. A. Migahed[1], A. M. Al-Sabagh[1], E. G. Zaki[1,*], H. A. Mostafa[2] and A.S. Fouda[2]

[1]Egyptian petroleum Research Institute, Nasr City, Cairo (11727), Egypt.

[2]Chemistry Department, Faculty of Science, Mansoura University, Egypt.

ARTICLE INFO

Article history:

Received: 29 October 2014;

Received in revised form:

22 November 2014;

Accepted: 2 December 2014;

Keywords

Corrosion inhibition, Carbon steel, Cationic surfactants, H_2S environment, EIS, Polarization , SEM, EDX.

ABSTRACT

Four new cationic surfactants based on sulphonamide were synthesized. Their chemical structures were confirmed using, FTIR, H NMR spectroscopic analyses. The surface active properties of the synthesized surfactants were calculated from surface tension measurements at different temperatures .The performance of these surfactants as corrosion inhibitors for X-65 type carbon steel in oil wells formation water under H_2S environment was investigated by potentiodynamic polarization and electrochemical impedance spectroscopy (EIS) techniques. The obtained results showed that the percentage inhibition efficiency (η%) was increased by increasing the inhibitor concentration until the critical micelle concentration (CMC) reached. Also, it was found that inhibition efficiency was increased by increasing both molecular size of the surfactant and introducing ethylene oxide units in the surfactant molecule. The data obtained from (EIS) was analyzed to model the corrosion inhibition process through equivalent circuit. Finally, the nature of the protective film formed on carbon steel surface was examined by SEM and EDX techniques.

Introduction

Corrosion inhibition of steel is an important issue both from industrial and scientific point of view. For instance in oil production countries worldwide, corrosion protection plays a vital role. Many cases of extensive corrosion have occurred in production tubing, valves, and flow lines from the wellhead to the processing equipment. One of the most important methods to inhibit corrosion of steel is to use adsorption inhibitors. This happens in many technological and practical areas such as acid pickling and descaling, petroleum industry storage of chemical in special tanks **[1,2].** Organic compounds bearing sulfur, oxygen or nitrogen heteroatom are widely used as corrosion inhibitors of steel in different media **[3–6].** This class of inhibitors exhibit high inhibition efficiency level at considerably low cost, in addition to their availability. Surfactants are one of the important categories which are widely applied as corrosion inhibitors for different metals such as Fe, Al and Cu in different media **[7, 8].** Surfactants exert their inhibition action through adsorption on the metal surface such that the polar or ionic group (hydrophilic part) attaches to the metal surface while its tail (hydrophobic part) extends to solution. The adsorption of surfactant on metal surface can markedly change the corrosion resisting property of the metal **[9, 10].**

Corrosion inhibitors, mainly surfactants, are widely employed in the petroleum industry to protect iron and steel equipment used in drilling, production, transport and refining of hydrocarbons **[11,12].** The efficiency of the inhibition film depends on inhibitor concentration and immersion time with metal surface. In fact, introducing of ethylene oxides into surfactant molecule (i.e. ethoxylation) increases the inhibitive effect of surfactant **[13],** Also the presence of these groups increases the solubility of surfactant and hence the extent of its adsorption on the metal surface increases, consequently its inhibitive action improves. Many studies on inhibition of the corrosion of carbon steel by some ethoxylated surfactants have been reported in different corrosive environment **[14–20]**.

It is well known that during the corrosion of carbon steel under H_2S environment, corrosion product film will formed on the steel surface according to the following reactions:

Anodic reaction:

$$Fe \rightleftharpoons Fe^{2+} + 2e \quad (1)$$

Cathodic reaction:

$$H_2S_{(aq)} + 2e \rightleftharpoons S^{2-} + H_2 \quad (2)$$

Overall reaction :

$$Fe + H_2S_{(aq)} \rightleftharpoons FeS + H_2 \quad (3)$$

Thus in the presence of H_2S, iron dissolution occurs forming ferrous sulfide as first corrosion product. This layer will be destroyed if high concentration of H_2S is present .

This work is aimed to examine corrosion inhibition efficiency of new synthesized surfactants on the corrosion rate of carbon steel in deep oil wells formation water under H_2S environment. It is an onset of a series of works currently under investigation in our labs.

Experimental

Chemical composition of X-65 type carbon steel alloy

X-65 type carbon steel specimens used in this investigation were cut from unused petroleum pipeline. The chemical composition(weight by weight) of carbon steel is C 0.09,Si 0.22 ,Mn 1.52 ,P 0.01 ,S 0.05, Ni 0.04 ,Cr 0.02 , Mo 0.004 ,V 0.002 ,Cu 0.02 , Al 0.04 and the reset is Fe.

Tele:

E-mail addresses: chemparadise17@yahoo.com

Deep oil well formation water

Deep oil wells formation water naturally exists in the reservoir rocks before drilling. Most oil field water contains a variety of dissolved organic and inorganic compounds. The major elements usually present are sodium, calcium, magnesium, chloride, bicarbonate and sulfate. The chemical composition of the oil wells formation water used in this investigation and its physical properties are shown in **Table 1.**

Synthesis of the inhibitors

Preparation of sulfonamide

Into 500 ml three-necked flask equipped with mechanical stirrer, condenser, Den-Stark Trap and Dropping funnel, 2 moles of Linear alkyl benzene sulphonic acid (LABS) was reacted with 1 diethylene triamine (DETA), triethylenetetramine, tetraethylene pentamine and pentaethylene hexamine in the presence of (100 ml) xylene as a solvent and 2% ZnO as a catalyst for 4 h reflux at 140 °C. Then, after complete removal of the theoretical amount of water of the reaction (36 ml), the solvent was stripped out using a rotary evaporator. The product dissolved in (30ml) isopropanol.

Ethoxylation of amide

In a 250 ml four-neck flask equipped with a condenser, magnetic stirrer, thermometer, ethylene oxide gas inlet and outlet nozzles ,2–3 droplets of triethylamine were added to 1 mole sulphonamide derivatives with stirring at 80–90 ^{0}C for about 15 min., then ethylene oxide gas was allowed to pass over the sulphonamide derivatives melt under a controlled pressure of around 86–88 cm Hg with stirring **[21-24].**

The temperature was raised gradually up to reflux temperature and then the reaction mixture was refluxed for about 3 h. After that it was cooled and flashed off every 0.5 h. The progress of the reaction was evaluated by monitoring the gained weight as a result of insertion of ethylene oxide units till reaching to the weight equivalent to insertion of ten ethylene oxide units to the sulphonamide derivatives.

Qaternarization

The preparation of some quaternary ammonium chloride by refluxing four mole of alkyl chloroide, namely: chloro dodecane with one mole of ethoxylated compounds in acetone as a solvent for 18h. The produced quaternary ammonium chloride was recrystallized three times in ethanol then washed with diethyl ether. Then 1 mole of potassium hydroxide in ethanol was refluxed with 1 mole of the produced quaternary ammonium bromide salts. The mixture was then cooled for 1h and filtered. The filtrate then was concentrated to yield quaternary ammonium chloride.

The chemical structure of the synthesized compounds are listed in **Scheme 1**.

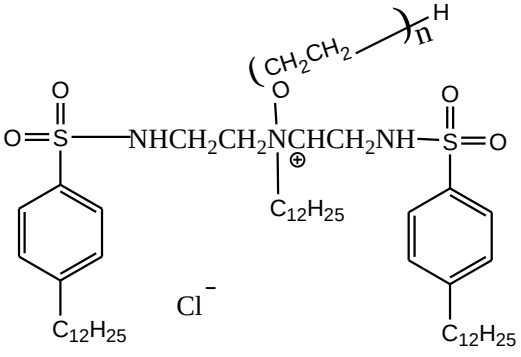

n=10e.o

(I)

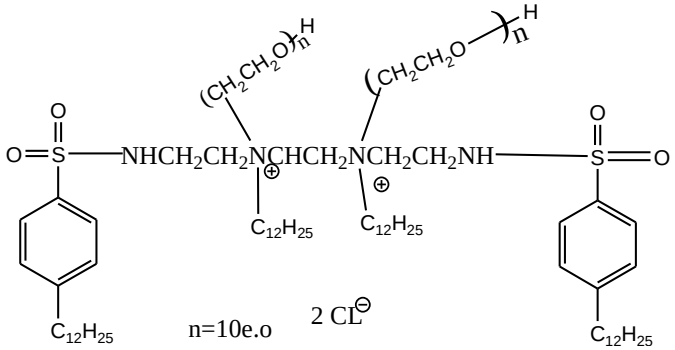

n=10e.o 2 $CL^{\ominus}$

(II)

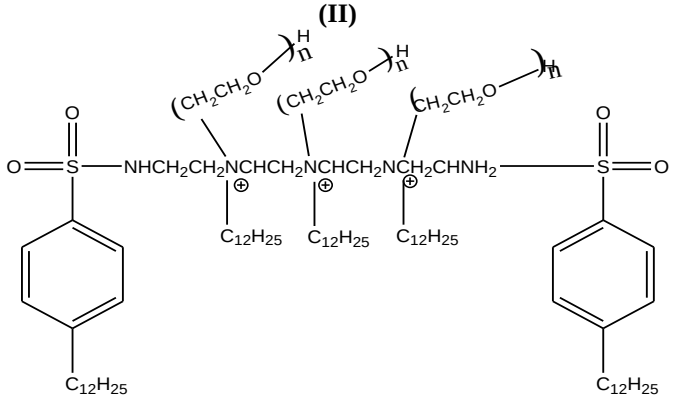

$3Cl^-$

n=10 e.o

(III)

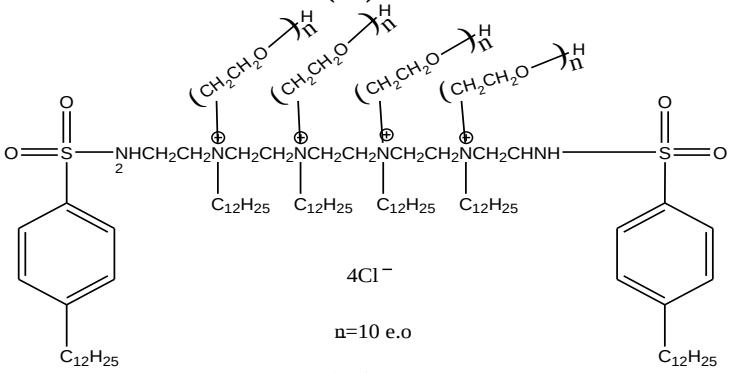

$4Cl^-$

n=10 e.o

(IV)

Scheme 1

FTIR spectroscopic analysis

The appearance of new characteristic absorption band for compound II at 3434.23 cm^{-1} assigned to the primary alcohol (–OH) of ethylene oxide units. The ethereal band (C–O–C) appeared at 1123.82 cm^{-1} which confirms that the ethoxylated derivatives were successfully prepared. **Fig. 1** shows the appearance of new characteristic absorption bands for compound IV at 2922.25 and 2857.57 cm^{-1} for the asymmetric and symmetric ($–CH_2$), 727 cm^{-1} for $(CH_2)_n$, 2900, 1303 cm^{-1} for CH_3, 1072, 655 cm^{-1} for the asymmetric and symmetric stretching N^+- C_4

^{1}H NMR spectrum spectroscopic analysis

All the above chemical shifts confirm the cationic compound IV was successfully prepared as showed in **Fig. 2** The chemical shifts at б (2.7) for ^{1}H proton (a) of the $–CH_2$ group in the first ethylene oxide unit attached to 3°rd N, the chemical shift б (3.8) for ^{1}H protons (b) $–CH_2$ group of repeated ethylene oxide units and the chemical shift at б (3.96) for ^{1}H protons (c) $–CH_2$ group of ethylene oxide unit near terminal (–OH). The chemical shifts at б (3.24) for ^{1}H proton of the $–CH_2$ group in the aliphatic group dodecyl.

The above chemical shifts confirm that the cationic derivatives were successfully prepared. The data of ^{1}H NMR

spectra confirmed the expected hydrogen proton distribution in the synthesized cationic surfactants.

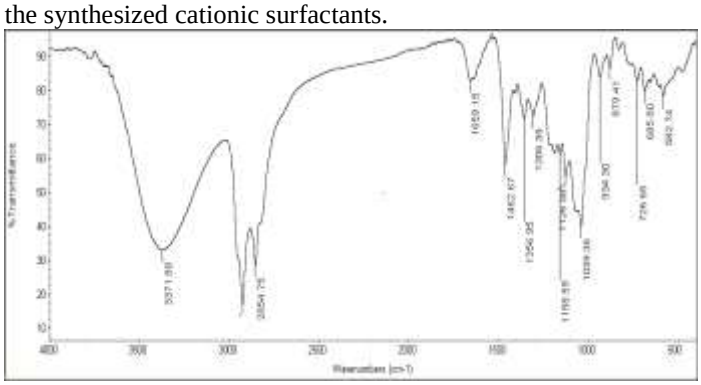

Figure 1: FTIR spectrum of compound IV

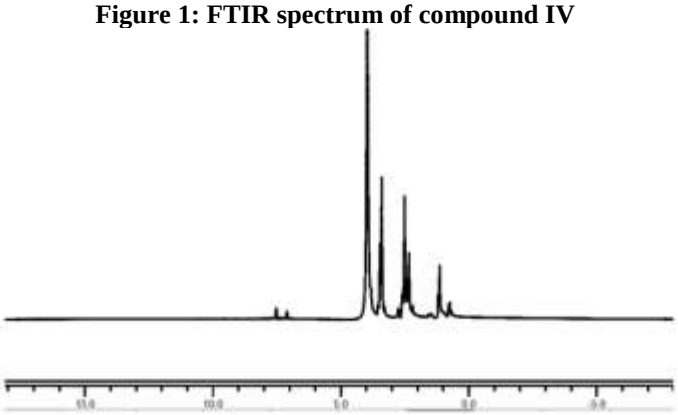

Figure 2: ^{1}H NMR spectrum of compound IV

Testing solution

The test solution for this work is deep oil formation water.H_2S gas was generated in situ by addition of equivalent amount of 0.5 M H_2SO_4 and 0.5 M Na_2S were prepared at first. The precise concentration of H_2S was determined by the iodometric titration method three times to make sure the results were reproducible and reliable.

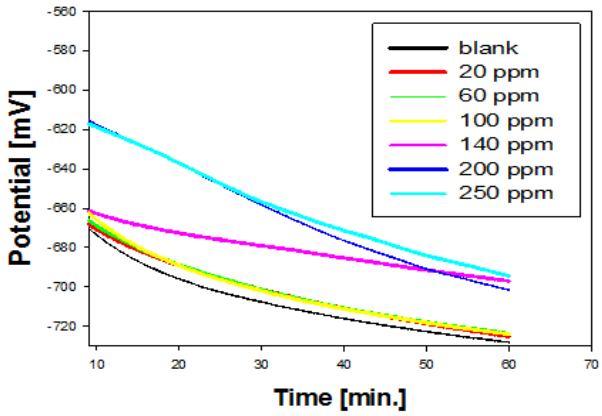

Figure 3. Potential–time curves for carbon steel in formation water in the absence and presence of various concentrations of the inhibitor (IV)

Open circuit potential measurements

All electrochemical experiments were carried out by Volta lab80 (Tacussel-radiometer PGZ402) controlled by Tacussel corrosion analysis software model (Volta master 4) attached to traditional three-electrode cell. The working electrode (WE) was a rod of API X65 steel pipeline embedded in PVC holder using epoxy resin so that the flat surface of the electrode (1.0 cm^2) was the only exposed area to the corrosive media the electrode was abraded with emery paper (grade 320–400–600–800–1000–1200) on the test face, rinsed with distilled water, degreased with acetone and dried.

A platinum electrode and a saturated calomel electrode (SCE) were used as auxiliary and reference electrode, respectively. All potential data reported were referred to SCE reference electrode. Before starting the experiments, the working electrode was immersed in test solution for 30 min at open circuit potential (OCP). All experiment were carried out at 298 k.

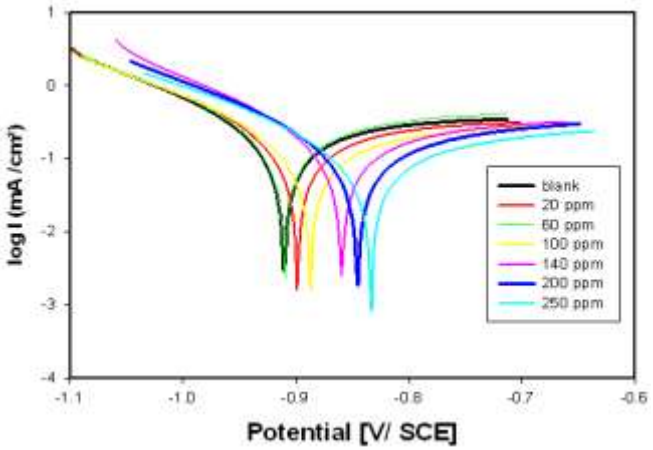

Figure 4. Potentiodynamic polarization curves (E – log I relationship) of carbon steel in formation water under H2S environment in the absence and presence of different concentrations of compound IV

Potentiodynamic polarization measurements

Polarization curves were recorded at a constant sweep rate of 2 mVs^{-1}. The values of corrosion current densities were calculated using Tafel extrapolation method by taking the extrapolation interval of 250 mV with respect to E_{corr}.

Electrochemical impedance spectroscopy (EIS)

Impedance spectra were obtained in the frequency range between 100 kHz and 50 mHz using 10 steps per frequency decade at open circuit potential after 3h of immersion time. AC signal with 20 mV amplitude peak to peak was used to perturb the system. EIS diagrams are given in Nyquist and Bode representations **[25].**

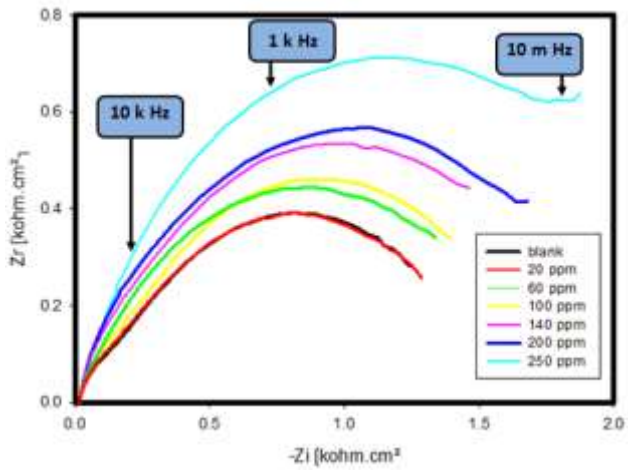

Figure 5: Nyquist plots for carbon steel in oil wells formation water in the absence and presence of different concentrations of compound IV

Surface tension measurements

The surface tension (γ) was measured using Kruss K6 Tensiometer type, a direct surface tension measurement, using ring method for various concentrations of the investigated surfactants.

Scanning electron microscopy

The surface examination was carried out using scanning electron microscope (JEOL JSM-5410, Japan). The energy of

acceleration beam employed was 20 kV. All micrographs were taken at a magnification power (X 1500).

Energy dispersive analysis of X-rays (EDX)

EDX system attached with a JEOL JSM-5410 scanning electron microscope was used for elemental analysis or chemical characterization of the film formed on carbon steel surface before and after applying the synthesized compound IV.

Results and discussion

Open circuit potential

The potential of carbon steel electrodes immersed in deep oil wells formation water were measured as a function of immersion time in the absence and presence of cationic inhibitor .It is clear that the potential of carbon steel electrode immersed in produced water from oil well (blank curve) tends towards more negative potential firstly in **fig. 3** as shown , giving rise to short step. This behavior represents the breakdown of the pre-immersion air formed oxide film presents on the surface according to the following equation:

$$Fe_2O_3 + 3H_2O \longrightarrow 2Fe(OH)_3 \quad (4)$$

This is followed by the growth of a new oxide film inside the solution , so that the potential was shifted again to more noble direction until steady state potential is established **[26].** Addition of inhibitor molecules to the aggressive medium produces a positive shift in the open circuit potential due to the retardation of the anodic reaction, which is the process of metal dissolution reaction.

Potentiodynamic polarization measurements

Figs. 4 show the cathodic and anodic polarization curves of carbon steel immersed in deep oil wells formation water under H_2S environment in the absence and presence of different concentrations of compound IV as a representative sample. Electrochemical parameters such as corrosion potential ($E_{corr.}$), corrosion current density ($i_{corr.}$), cathodic and anodic Tafel slopes (b_c and b_a) were calculated. From the obtained polarization curves, it is clear that the corrosion current densities ($i_{corr.}$) were decreased with increasing concentration of compound IV with respect to the blank (inhibitor free solution). These results greatly agree and confirm the formation of a good protective layer on the surface of carbon steel. The degree of surface coverage (θ) and the percentage inhibition efficiency (η%) were calculated using the following equations **[27]:**

$$\theta = 1 - \frac{i}{i_o} \quad (5)$$

$$\eta\,\% = (1 - \frac{i}{i_o}) \times 100 \quad (6)$$

where i_0 and i are the corrosion current densities in the absence and presence of the inhibitor, respectively.

A careful inspection of the polarization curves indicated that Tafel lines are shifted to more negative and more positive potentials for the anodic and cathodic processes, respectively relative to the blank curve. This means that the selected compound acts as mixed type inhibitor, i.e., promoting retardation of both anodic and cathodic discharge reactions. Complete data obtained from polarization measurements are summarized and listed in **Table 2**. The results indicate that the percentage inhibition efficiency (η%) of compound IV is greater than that of compounds III , II. and I This could be attributed to the application of along chain alkyl halide which promotes stronger adsorption film and hence more protective layer and higher inhibition efficiency.

The anodic Tafel slope (ba) and cathodic Tafel slope (bc) of the used cationic surfactants were slightly changed with inhibitor concentrations; this indicates that these inhibitors affected both the anodic and cathodic reactions **[28]** by the slight change upon increasing inhibitor concentrations indicating that the presence of prepared cationic surfactants don't change the reaction mechanism of inhibition **[29].** The adsorption of inhibitors can affect the corrosion rate in two ways: (i) by decreasing the available reaction area, the so-called geometric blocking effect, and (ii) by modifying the activation energy of the cathodic and/or anodic reactions occurring in the inhibitor-free metal in the course of the inhibited corrosion process. Theoretically, no shifts in E_{corr} should be observed after addition of the corrosion inhibitor if the geometric blocking effect is stronger than the energy effect **[30].** The change observed in the E_{corr} values upon addition of cationic surfactants indicates that the energy effect is stronger than geometric blocking effect **[31].** The addition of inhibitors shifts the E_{corr} values towards the positive since the largest displacement does not exceed 80 mV at 25 ^{0}C as shown in **Table 2**; it may be concluded that theses inhibitors act as a mixed-type (anodic/cathodic) inhibitors with a predominantly anodic reaction meaning inhibitors reduce the anodic dissolution of mild steel and also retards the cathodic hydrogen evolution reaction but the effect on the anodic dissolution reactions is more than on the cathodic hydrogen evolution reactions.

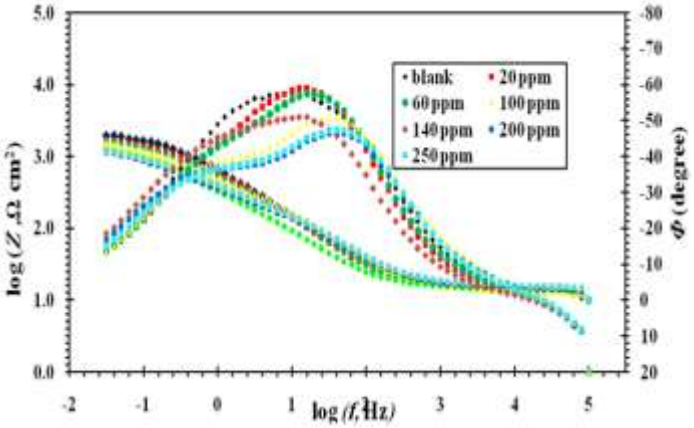

Figure 6: Bode plots for the carbon steel in the oil wells formation water in the absence and presence of various concentrations of inhibitor (IV)

Electrochemical impedance spectroscopy (EIS)

The corrosion behavior of carbon steel in deep oil wells formation water under H_2S environment in the absence and presence of various concentrations of compound IV as a representative sample was investigated by EIS technique. Nyquist and Bode plots is shown in **Figs. 5&6** It is clear from plots that the impedance response of carbon steel in formation water was significantly changed after the addition of the inhibitor molecules. Various parameters such as the charge transfer resistance R_t, double layer capacitance C_{dl} and percentage inhibition efficiency η% were calculated according to the following equations and listed in **Table 3**. The values of R_t were given by subtracting the high frequency impedance from the low frequency one as follows **[32]:**

$$R_t = Z'_{re.}(at\ low\ frequency) - Z'_{re.}(at\ high\ frequency) \quad (7)$$

The values of C_{dl} were obtained at the frequency f_{max} ,at which the imaginary component of the impedance is maximal-Z_{max} using the following equation:

$$C_{dl} = \frac{1}{2\pi f_{max}} \frac{1}{R_t} \quad (8)$$

and percentage inhibition efficiency η% were calculated from the values of R_t using the following equation:

$$\eta\% = \left[1 - \frac{R_t}{R_{t(inh)}}\right] \times 100 \quad (9)$$

where R_t and $R_{t(inh.)}$ are the charge transfer resistance values in the absence and presence of inhibitor, respectively. Increasing the value of charge transfer resistance (R_t) and decreasing the value of double layer capacitance (C_{dl}) by increasing the inhibitor concentration indicate that the surfactant molecules inhibit corrosion rate of carbon steel in deep oil wells formation water by adsorption mechanism **[33].** For analysis of the obtained impedance spectra, the equivalent circuit (EC) was obtained using Boukamp program as shown in **Fig. 7,** where $\mathbf{R_S}$ is the solution resistance , $\mathbf{R_t}$ is the charge transfer resistance ,$\mathbf{C_{dl}}$ is the electrochemical double layer capacitance **[34]** , $\mathbf{R_f}$ is the film resistance and $\mathbf{C_f}$ is the film capacitance. From EIS data it was found that the percentage inhibition efficiency of compound IV is greater than that of compounds III , II and I. Thereby, agreeing with aforementioned results potentiodynamic polarization measurements.

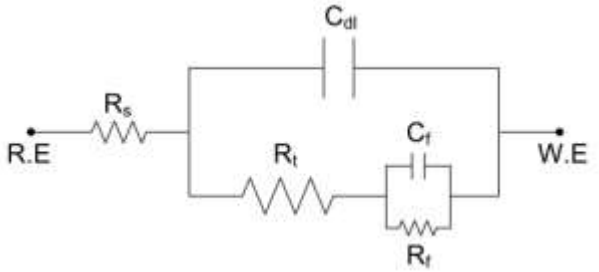

Figure 7: Equivalent circuit used to model impedance data of carbon steel in oil well formation water under H_2S environment

The electrochemical impedance parameters derived from the Nyquist plots and the inhibition efficiency (η%) were listed in **Table 3;.** It is observed from these plots that the impedance response of carbon steel in uninhibited solution changes significantly after addition of prepared cationic surfactant in the corrosive solution; as a result, real axis intercept at high and low frequencies in the presence of inhibitor(inhibited solution) is larger than that in the absence of inhibitor (blank solution). Also as the inhibitor concentration increased, the R_{ct} values increased and the C_{dl} values tended to decrease due to a decrease in local dielectric constant and/or an increase in the thickness of the electrical double layer suggesting that the inhibitor molecules acted by adsorption at the metal/solution interface. Addition of synthesized inhibitors provided lower C_{dl} values probably as a consequence of replacement of water molecules by inhibitor molecule at the electrode surface.

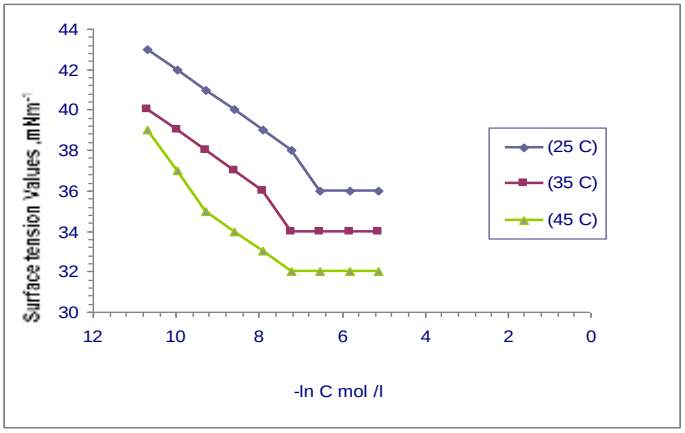

Figure 8: Surface tension vs. log C of compound IV at different temperatures

C_{dl} value was always smaller in the presence of the inhibitor than in its absence which may be resulted from the effective adsorption of the synthesized inhibitors on the electrode surface. Electrochemical impedance spectroscopy and polarization measurements were repeated several times and were observed that they were highly reproducible. The results obtained from EIS measurements are in good agreement with that obtained from both potentiodynamic polarization measurements.

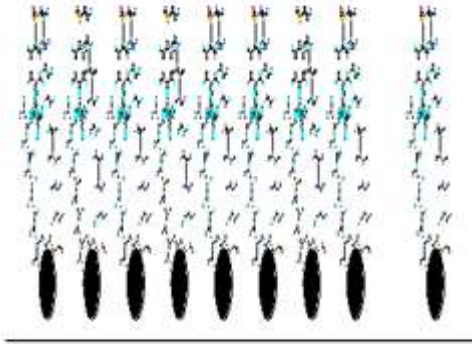

(a)

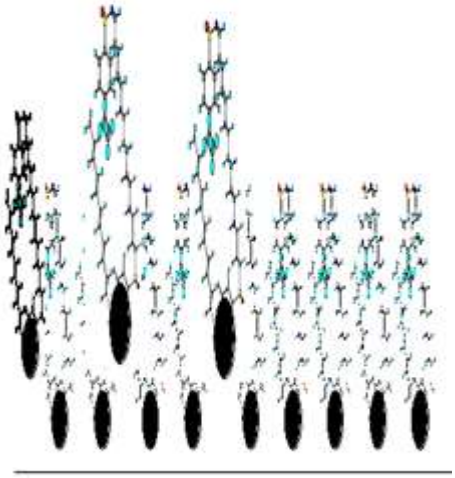

(b)

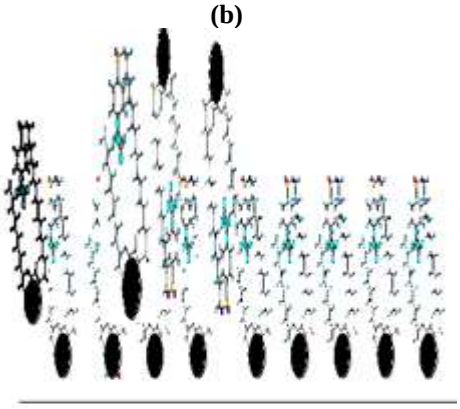

(c)

Figure 9. Schematic representation of the inhibitor adsorption on carbon steel surface. (a) Adsorption as single molecule at low concentration. (b) Hemimicelle formation at higher concentration. (c) Formation of multi-layers at very high concentration

Effect of hydrophobic chain length

The data in **Tables 2,3** reveal that increasing the hydrophobic chain length has an enhancing effect on the increasing of the corrosion inhibition. This is due to the presence of these chains which can do more successive protective layers on the metal surface; this leads to get rid of the corrosive species away from the metal surface and decrease the corrosion process. Also, the repulsion between the polar corrosive medium and

these nonpolar chains decreases the interaction and consequently decreases the corrosion processes occurred for these surfaces.

Effect of hydrophilic group (head group)

The adsorption of the inhibitor molecules on the mild steel surface can be explained on the basis of the donor acceptor interaction between p electrons of donor groups and aromatic rings of the inhibitors, and the vacant d orbitals of iron surface atoms **[35,36].** With an increase in the electron density at the reaction center, the chemisorption bonds between the inhibitor and the metal are strengthened **[37,38].**

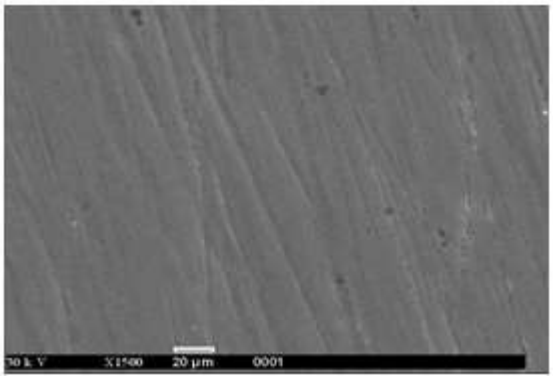

(a)

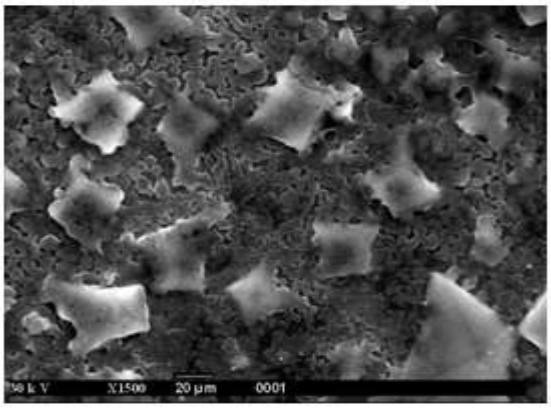

(b)

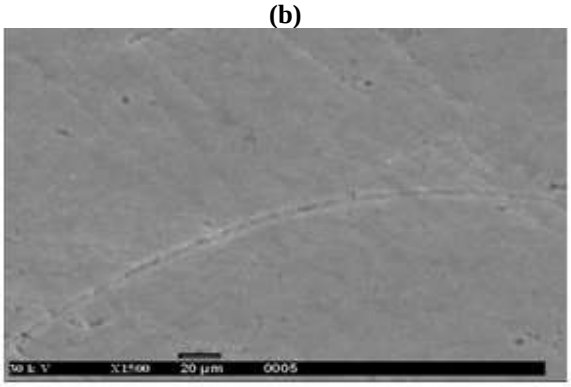

(c)

Figure 10: SEM of the carbon steel surface: (a) polished sample, (b) after immersion in the formation water and (c) after immersion in the formation water in the presence of 250 ppm of compound IV

Surface tension measurements

The CMC values of the synthesized surfactants were determined at various temperatures from the change in the slope of the plotted data of surface tension (γ) versus the natural logarithm of the solute molar concentration; ln C, as shown in **Fig. 8**. The data obtained from surface tension are summarized and listed in **table 4**.

The critical micelle concentration (CMC) is the point in concentration at which it becomes thermodynamically favorable for surfactant molecules in solution to form aggregates (micelles) in order to minimize interaction of either their head groups or their tail groups with the solvent. For the under investigation poly ethoxylated nonionic surfactant and cationic molecules in water, micellization is due to entropic considerations. Water molecules in close proximity to the hydrophobic group of the surfactant molecules take on a certain ordered configuration which is entropically unfavorable. Once the surfactant concentration reaches a certain level (CMC), the water structure forces aggregation of the hydrophobic tail groups forming surfactant micelles as illustrated in the schematic diagram **Fig. 9.**Surface tension plots indicate that each surfactant is molecularly dispersed at low concentration, leading to a reduction in surface tension until certain concentration is reached the surfactant molecules form micelles, which are in equilibrium with the free surfactant molecules.

Free energy of micellization vs. free energy of adsorption

Free energy of micellization (ΔG_{mic}) for the investigated surfactants was calculated from the following equation **[39]:**

$$\Delta G_{mic} = RT \ln CMC \qquad (10)$$

The obtained values of free energy of micellization (ΔG_{mic}) and free energy of adsorption (ΔG_{ads}), as summarized in **Table 5**, indicated that compound I with the lowest molecular weight favors micellization rather than adsorption as comparing to compound III with introducing of ethylene oxide units and long chain. This proves that compound III forms the strongest adsorption film on the metal surface and hence the maximum inhibition efficiency, which emphasizes that the inhibition efficiencies of the synthesized inhibitors increase in the following order as predicted by the different techniques: potentiodynamic polarization and electrochemical impedance spectroscopy. compound I < compound II < compound III < compound IV.

Effect of inhibitor concentration

At low surfactant concentrations the adsorption takes place by binding to hydrophobic region as seen in **fig 9.a.** In other words, a mono disordered layer may be formed. This adsorption was a competitive one because the inhibitor displaces progressively the water molecules and other ions adsorb on the metal surface. When surfactant concentration increases, un-complete packing layer of the inhibitor molecules was formed in which adsorption takes place as a result of an inter-hydrophobic chain interactions which clear in **fig 9.b.** In other words, the increase in inhibition efficiency observed at higher inhibitor concentrations indicates that more inhibitor molecules were adsorbed on the metal surface, thus providing wider surface coverage **[40].**Meanwhile at the over dose concentration (at maximum inhibition efficiency obtained), the inter space area between the adsorbed inhibitor molecules on the surface may be lesser than the area of the inhibitor molecules. So that, the inhibitor molecules turn out to form the double layer adsorption as shown in **fig 9.c.**

Scanning electron microscopy (SEM)

Fig. 10a shows SEM image of polished carbon steel surface. The micrograph shows a characteristic inclusion, which was probably an oxide inclusion **[41]. Fig. 10b** shows SEM of the surface of carbon steel specimen after immersion in formation water for 70 days in absence of inhibitor, while **Fig. 10c** shows SEM of the surface of another carbon steel specimen after immersion in formation water for the same time interval in the presence of 250 ppm of the compound IV. The resulting scanning electron micrographs reveal that, the surface was strongly damaged in the absence of the inhibitor, but in the presence of 250 ppm of the compound IV, there is less damage

in the surface. This confirms the observed high inhibition efficiency of compound IV at this concentration.

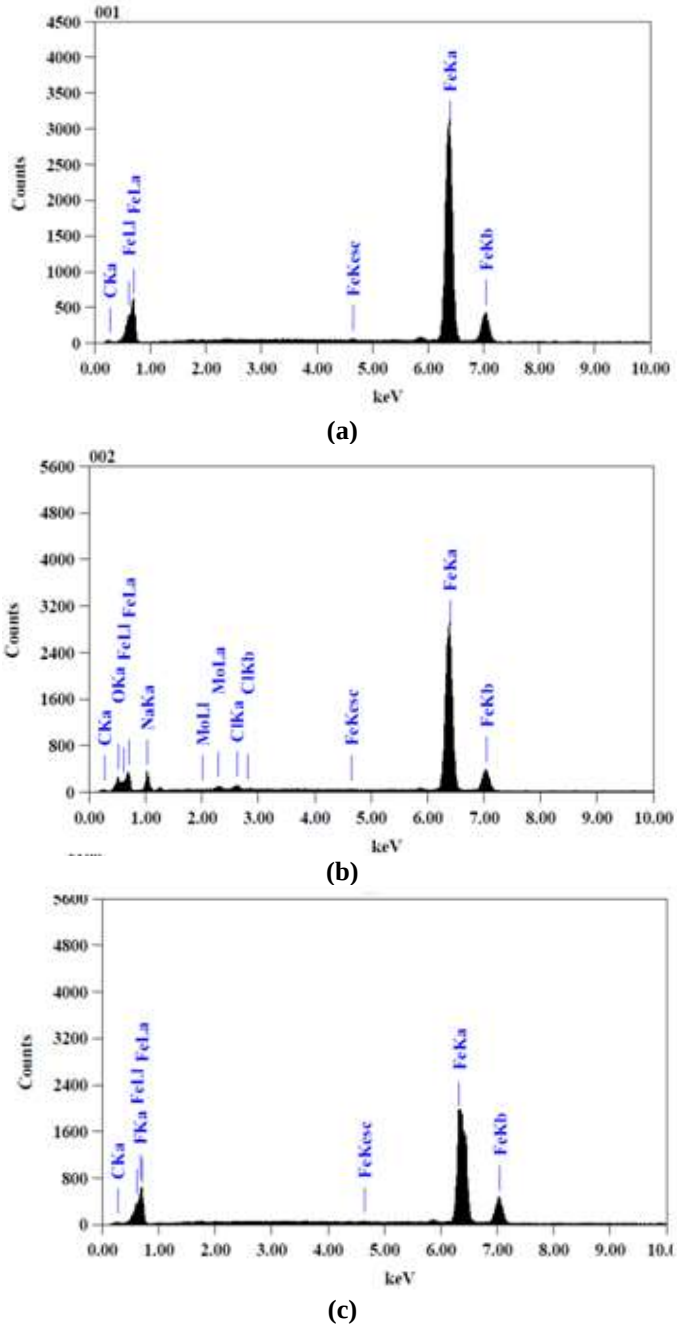

Figure 11: EDX of the carbon steel surface: (a) polished sample, (b) after immersion in the formation water and (c) after immersion in the formation water in the presence of 250 ppm of compound IV

Energy dispersive analysis of X-rays (EDX)

The EDX spectrum in **Fig. 11a** shows the characteristic peaks of some elements constituting the polished carbon steel surface. The spectrum of the polished carbon steel surface after immersion in the formation water in the absence and presence of compound IV for 70 days, is shown in **Figs. 11b and 11c** ,respectively. The spectrum of **Fig. 11c** shows that the Fe peak is considerably decreased relative to the samples in **Figs. 11a** and **11b**. This decreasing of the Fe band is indicated that strongly adherent protective film of compound IV formed on the polished carbon steel surface, which leads to a high degree of inhibition efficiency **[42].** The oxygen signal apparent in **Fig. 11b** is due to the carbon steel surface exposed to the formation water in the absence of compound IV. Therefore, EDX and SEM examinations of carbon steel surface support the results obtained from chemical and electrochemical methods that the synthesized surfactant inhibitors are a good inhibitors for carbon steel in oil wells formation water.

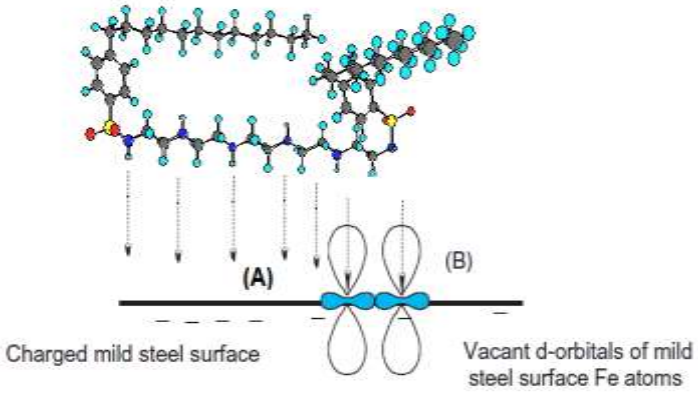

Figure 12. **Types of interaction between the inhibitor cations and mild steel surface (dipole adsorption model: (A) physical adsorption and (B) chemisorptions)**

Inhibition mechanism

The adsorption of organic molecules on the solid surfaces may be physisorption or chemisorption or a mixture of both processes.

In physical adsorption, inhibitor molecules can also be adsorbed on the steel surface via electrostatic interaction between the charged metal surface and the charged inhibitor molecule. Chemical adsorption of the inhibitors arises from the donor acceptor interactions between the free electron pairs of heteroatoms and p-electrons of multiple bonds as well as a phenyl group and vacant d-orbitals of iron **[43,44].** The orientation of molecules may depend on the pH and/or electrode potential **[45].** In the case of parallel adsorption of inhibitor molecules, the steric factors also must be taken into consideration. The adsorption free energy values are ranged between ⁻17 and ⁻30 kJ mol^{-1} which indicate that the adsorption mechanism of the prepared quaternary ammonium compounds on for X-65 type carbon steel in oil wells formation water under H_2S environment is a mixed of physical and chemical adsorption**.** The tested inhibitors exist either as neutral or in the form of cationic molecules. The inhibitors may adsorb on the Metal/acid solution interface by one or more of the following ways: (i) electrostatic interaction of protonated forms of the inhibitor molecules with the adsorbed ions,(ii) donor–acceptor interactions between the p-electrons of phenyl ring and vacant d-orbital of surface Fe atoms,(iii) interaction between unshared electron pairs of the oxygen atoms in the polyoxyethylene chains and the vacant d-orbital of Fe surface atoms. Hence, the adsorption modes of the inhibitors can be considered either by the neutral molecules or by the cationic forms.In case of neutral molecules adsorption mode, the molecules can be adsorbed on the surface of carbon steel through the chemisorptions mechanism. That occurred by the displacement of the adsorbed water molecules from the metal surface and the sharing electrons between the hetero atoms and iron. Furthermore, inhibitor molecules adsorb on the metal surface by the donor–acceptor interactions between p-electrons of the phenyl ring of species and vacant d-orbitals of Fe atoms. it is well known that the steel surface bears positive charge in acid solution **[46],** The schematic illustration of different modes of adsorption on metal/acid interface is shown in Fig. **12 [47].**

Table 1: Chemical composition and physical properties of deep oil well formation water used in this investigation

Physical properties	Unit	Value
Density	g/cm^3	1.044
Turbidity	FAU	263
PH		6.38
Salinity NaCl	mg/l	12029
Conductivity	µs/cm	29220
Total hardness	mg/l	2910
Ionic species		Value
Sulfate	(mg/l)	6.5
Phosphate	(mg/l)	0.771
Bi-carbonte	(mg/l)	143
Chloride	(mg/l)	7300
Sulfide	(mg/l)	450
Iron ferrous	(mg/l)	23
Iron, total	(mg/l)	42
Calcium	(mg/l)	800
Magnesium	(mg/l)	364
Barium	(mg/l)	105
Potassium	(mg/l)	250
ZINC	(mg/l)	1.359
TDS	(mg/l)	15520

Table 2: data obtained from potentiodynamic polarization measurements of carbon steel in formation water solution in the absence and presence of various concentrations of compounds I, II and III,IV at 298 K.

Inhibitor	Conc., ppm	$-E_{corr}$, mV vs. SCE	I_{corr}, µA/cm²	b_a, mV dec^{-1}	$-b_c$, mV dec^{-1}	η%
I	0	942.9	0.3503	87.9	136.6	-
	20	926.5	0.1990	84.1	140.2	43.19
	60	940.8	0.1905	70.5	146.2	45.61
	100	913.5	0.1893	73.5	117.0	45.96
	140	946.4	0.1885	78.2	105.7	46.61
	200	944.8	0.1843	64.3	110.1	47.38
	250	949.6	0.1761	71.9	102.4	49.72
II	20	919.1 mV	0.2013	85.8	137.5	42.53
	60	964.4 mV	0.2043	70.5	146.2	44.73
	100	920.5mV	0.1559	73.9	121.8	55.49
	140	918.9mV	0.1460	71.1	138.5	58.32
	200	895.1 mV	0.0930	68.2	153.6	73.45
	250	841.7mV	0.0773	68.1	131.4	77.93
III	20	955.6	0.1996	84.4	131.7	43.02
	60	964.4	0.1791	73.4	120.6	48.87
	100	910.0	0.1936	74.6	128.7	59.06
	140	887.2	0.1144	71.8	135.6	73.33
	200	900.4	0.0534	70.6	130.4	84.75
	250	845.4	0.0353	70.1	117.8	89.91
IV	20	955.6	0.1979	85.2	130.3	43.50
	60	964.4	0.1891	72.4	120.7	46.87
	100	910.0	0.1464	73.6	128.6	58.06
	140	887.2	0.1044	70.8	133.4	70.33
	200	900.4	0.0583	69.6	130.4	83.75
	250	845.4	0.0343	68.4	110.8	90.20

Table 3: data obtained from electrochemical impedance spectroscopy (EIS) measurements of carbon steel in formation water solution in the absence and presence of various concentrations of compounds I, II ,III and IV

Inhibitor	Conc., ppm	coefficient	R_f, kΩcm^2	C_f, µF/cm^2	R_t, kΩcm^2	C_{dl}, µF/cm^2	η %
I	0	0.98	----	----	3.40	124.	---
	20	0.99	0.28	50.1	5.50	93.58	38.18
	60	0.98	0.35	45.2	6.94	89.92	50.7
	100	0.96	0.42	39.6	9.31	85.38	63.44
	140	0.97	0.45	33.5	10.47	68.01	67.52
	200	0.99	0.48	25.6	12.0	59.71	71.66
	250	0.98	0.50	23.7	13.1	39.91	74.04
II	20	0.99	0.33	52.2	5.6	46.13	39.28
	60	0.96	0.37	46.2	7.15	46.13	52.44
	100	0.97	0.44	40.5	9.7	39.93	64.95
	140	0.99	0.47	34.5	11.1	37.59	69.36
	200	0.98	0.49	28.2	13.0	29.01	73.85
	250	0.96	0.52	26.8	14.5	15.34	76.55
III	20	0.98	0.32	53.1	5.9	52.52	42.37
	60	0.97	0.38	47.3	8.19	43.36	58.48
	100	0.96	0.45	41.7	9.74	39.90	64.94
	140	0.98	0.48	35.6	11.7	36.18	70.9
	200	0.99	0.51	28.4	13.63	31.93	75.05
	250	0.98	0.53	27.2	17.9	28.35	81.00
IV	20	0.96	0.33	53.3	6.11	52.7	44.35
	60	0.97	0.35	47.5	8.3	43.47	59.0
	100	0.96	0.45	41.9	9.76	40.1	65.1
	140	0.98	0.49	35.8	12.1	36.3	71.9
	200	0.99	0.52	28.7	13.9	32.2	75.5
	250	0.98	0.55	27.5	18.2	28.8	81.31

Table 4: Surface active properties of the synthesized compounds I, II.III and IV

Corrosion Inhibitor	Temp	CMC mole/dm^3	γ_{cmc}mN/m	Γ_{max} x10^{-7}, mol/m^{-2}	A_{min},nm^2	Π_{CMC}	ΔG_{mic}Kj/mol^{-1}	ΔG_{ads}Kj/mol^{-1}
I	25°C	3.48 x10^{-3}	36	1.07x10^{-10}	154	36.3	-14.02	-17.41
	35°C	1.75x10^{-3}	34	1.15x10^{-10}	144	38.3	-16.26	-19.58
	45°C	8.76x10^{-4}	33	1.17x10^{-10}	141	39.3	-18.61	-21.96
	55°C	7.77x10^{-4}	31	7.8x10^{-11}	212	41.3	-21.18	-26.47
II	25°C	3.28x10^{-3}	35	6.39 x10^{-11}	259	37.3	-14.17	-20.00
	35°C	1.65x10^{-3}	34	4.67x10^{-11}	355	38.3	-16.41	-24.60
	45°C	8.25x10^{-4}	30	6.66x10^{-11}	248	42.3	-18.77	-25.11
	55°C	4.14x10^{-4}	29	6.66x10^{-11}	248	43.3	-21.24	-27.73
III	25°C	7.77x10^{-4}	35	7.35x10^{-11}	226	37.3	-17.44	-22.81
	35°C	7.77x10^{-4}	34	4.6x10^{-11}	357	38.3	-18.33	-26.57
	45°C	3.90x10^{-4}	32	3.8x10^{-11}	435	40.3	-20.75	-31.31
	55°C	2.01x10^{-4}	31	3.4x10^{-11}	483	41.3	-23.20	-35.23
IV	25°C	1.49x10^{-3}	36	7.8x10^{-11}	300	36.3	-16.13	-22.70
	35°C	7.47x10^{-4}	34	6.9x10^{-11}	348	38.3	-18.43	-26.47
	45°C	3.71x10^{-4}	32	6.2x10^{-11}	348	40.3	-20.88	29.34
	55°C	1.86x10^{-4}	31	5.2x10^{-11}	418	41.3	-23.42	-33.82

Table 5. Standard free energy of micellization (ΔG_{mic}) and standard free energy of adsorption (ΔG_{ads}) as obtained from surface tension measurements

Corrosion Inhibitor	Temp.	Free energy of micellization ΔG_{mic} (kJ mol^{-1})	Free energy of adsorption ΔG_{ads}(kJ mol^{-1})
I	25°C	-14.02	-17.41
	35°C	-16.26	-19.58
	45°C	-18.61	-21.96
II	25°C	-14.17	-20.00
	35°C	-16.41	-24.60
	45°C	-18.77	-25.11
III	25°C	-17.44	-22.81
	35°C	-18.33	-26.57
	45°C	-20.75	-31.31
IV	25°C	-16.13	-22.70
	35°C	-18.43	-26.47
	45°C	-20.88	29.34-

Conclusions

In this study, the inhibition properties for (I-IV) are tested by using electrochemical measurements(OCP, potentiodynamic polarization and EIS). According to the results, Compound IV is good inhibitor in oil well formation water under H_2S environment than (I,II,III)group I owing to alkyl chain within the molecule in Compound IV. Polarization curves showed that the inhibitor is a mixed type one. The protection efficiency increased with increasing inhibitor concentration. The decrease in the capacitance double layer (C_{dl}) with concentration indicated that, the studied compounds are adsorbed on the metal surface creating a physical barrier to charge and mass transfer for metal dissolution .Selection of these compounds as corrosion inhibitors was based on the facts that these compounds contain lone pair of electrons on the N and p electrons in the aromatic ring through which it can adsorbed on the metal surface .The lateral interaction of the long chain of carbon atoms due to Vander Waals forces can further facilitate formation of compact film of the inhibitor on the metal surface .As a representative type of these quaternary ammonium salts have been demonstrated to be highly cost-effective and used widely in various industrial processes for preventing corrosion of iron and steel in acidic media. The critical micelle concentration considers a key factor in determining the effectiveness of surfactants as corrosion inhibitors due to large reduction of surface tension at CMC .the inhibition mechanism is attributed to the strong adsorption ability of the selected surfactants on carbon steel surface, forming a good protective layer, which isolates the surface from the aggressive environment. The formation of a good protective film on carbon steel surface was confirmed using SEM and EDX technique.

Acknowledgments

This work has been financially supported by Egyptian Petroleum Research Institute (EPRI) fund. The authors are greatly thanked to EPRI fund and support

References

[1] Rosenfeld IL. Corrosion inhibitors. London: Springer-Verlag; 2004, p. 326–8.

[2] Mansfeld F. Corrosion inhibitors. New York: Marcel Dekker; 1978, p. 742–4.

[3] Emregu'I KC, Akay AA, Atakol O, Mat Chem Phys 2005;93:325–9.

[4] Qiu LG, Xie AJ, Shen YH. Corros Sci 2005;47:273–8.

[5] Noor EA.Corros Sci 2005;47:33–55.

[6] Atia AA, Saleh MM. J Appl. Electrochem 2003;33:171–7.

[7] Lake DL. Approching environmental acceptability in cooling water corrosion inhibition. Corros. Prevent. Control 1988:113–4.

[8] Sastri VS. Corrosion inhibitors; principles and applications. NY: John Wiley and Sons; 1998, p. 198–202.

[9] Free ML. Corros Sci.2002;44:2865–70.

[10] Li X, Deng S, Fu H. J Appl Electrochem 2011;41:507–17.

[11] M. Elachouri, M.S. Hajji, S. Kertit, E.M. Essassi, M. Salem, R. Coudert,(1994) Corros. Sci.,37 : 381.

[12] Z. Wei, P. Duby, P. Somasundaran,(2003) J. Colloid Interf. Sci. ,259 : 97.

[13] J.H. Clint, (1992)Surfactant Aggregation, Blackie/Chapman & Hall, Glasgow and London/New York.

[14] A.J. McMahon,(1991) Colloids Surf. ,59 : 187.

[15] M.M. Osman, A.M.A. Omar, A.M. Sabagh,(1997) Mater. Chem. Phys., 50 : 271.

[16] F. Hanna, G.M. Sherbini, Y. Brakat, (1989) Corros. J., 24 : 269.

[17] M.M. Osman, M.N. Shalaby, (2002)Mater. Chem. Phys. ,77 : 261.

[18] A.M. Alsabagh, M.A. Migahed, Hayam S. Awad,(2006) Corros. Sci., 48 :813.

[19] M.A. Migahed, M. Abd-El-Raouf, A.M. Al-Sabagh, H.M. Abd-El-Bary,(2005) Electrochim. Acta, 50 : 4683.

[20] M.A. Migahed, H.M. Mohamed, A.M. Al-Sabagh, (2003) Mater. Chem. Phys. ,80 :169.

[21] W. Hreczuch, A. Kozlek,(1996) Tens. Surf. Det. ,38 (2) :621.

[22] W. HrecZuch, A. Kozlek, (1996)Tens. Surf. Det. ,38 :621.

[23] N.M. Van Os,(1998) Non-Ionic Surfactant ''Organic Chemistry'', Surfactant Science Series, vol. 72, Marcel Dekker, New York.

[24] R.F. Lang, P.D. Diaz, D. Jocobs,(1999) J. Surf. Det. ,7 :503.

[25] S. Liu, N. Xu, J. Duan, Z. Zeng, Z. Feng, R. Xiao, Corros. Sci. 51 (2009) 1356–1363.

[26] K.C. Emregul, M. Hayvali, Corros. Sci. 4 38 (2006) 797–812.

[27] Q.B. Zhang, Y.X. Hua,(2009) Electrochim. Acta ,54 : 1881.

[28] F.G. Liu, M. Du, J. Zhang, M. Qiu, Corros. Sci. 51 (2009) 102–109. **[29]** Xianghong Li, Shuduan Deng, Hui Fu, Corros. Sci. 55 (2012) 280–288.

[30] F.S. de Souza, Corros. Sci. 51 (2009) 642–649.

[31] Y. Ahmed, Musa, H. Abdul Amir, Kadhum, Abu Bakar Mohamad, Mohd Sobri Takriff, Abdul Razak Daud, Siti Kartom Kamarudin, Corros. Sci. 52 (2010) 526– 533.

[32] A.P. Yadav, A. Nishikata, T. Tsuru,(2004) Corros. Sci. ,46 : 169.

[33] K.F. Khaled,(2006) Appl. Surf. Sci., 252 : 4120.

[34] L. Larabi, Y. Harek, M. Traisnel, A. Mansri, J. Appl. Electrochem. 34 (2004) 833–839.

[35] F. Bentiss, M. Traisnel, M. Lagrence, Appl. Surf. Sci. 161 (2000) 196.

[36] R.A. Prabhu, T.V. Venkatesha, A.V. Shanbhag c, G.M. Kulkarni, R.G. Kalkhambkar, Corros. Sci. 50 (2008) 3356–3362.

[37] R.R. Annand, R.M. Hurd, N. Hackerman, J. Electrochem. Soc. 112 (1965) 1968.

[38] E.Z. Cook, N. Hackerman, J. Phys. Chem. 55 (1951) 549.

[39] J. Rosen,(2004) Milton Surfactants and Interfacial Phenomena, third ed., John Wiley & Sons Inc.

[40] G. Avci, Colloids Surf. A Physicochem. Eng. Aspects 317 (2008) 730–736.

[41] G.Y.Elewady,I.A.El-said,A.S.fouda, (2008)int.J. Electrochem.sci, 3 : 172-190.

[42] M. A. malik,M. A. Hashim,f. Nabi,S. A. Al-thabaiti,Z. khan,(2011) int.J. Electrochem.sci, 6 : 1927-1948.

[43] M. Behpour, S.M. Ghoreishi, M. Salavati-Niasari, B. Ebrahimi, Mater. Chem. Phys. 107 (2008) 153–157.

[44] A. Yurt, A. Balaban, S. UstunKandemir, G. Bereket, B. Erk, Mater. Chem. Phys. 85 (2004) 420–426.

[45] L. Vracar, D.M. Drazic, Corros. Sci. 44 (2002) 1669–1680.

[46] G.N. Mu, T.P. Zhao, M. Liu, T. Gu, Corrosion 52 (1996) 853.

[47] I. Ahamad, R. Prasad, M.A. Quraishi, Corros. Sci. 52 (2010) 1472–1481.